6. W. H. Schlesinger, *Biogeochemistry: An Analysis of Global Change* (Academic Press, San Diego, CA, 1991).
7. M. V. Thompson, J. T. Randerson, C. M. Malmström, C. B. Field, *Global Biogeochem. Cycles* **10**, 711 (1996).
8. N. Gruber, J. L. Sarmiento, T. F. Stocker, *ibid.*, p. 797.
9. C. T. Tynan, *Nature* **392**, 708 (1998).
10. S. J. McNaughton, *ibid.* **345**, 613 (1990).
11. M. Behrenfeld and P. Falkowski, *Limnol. Oceanogr.* **42**, 1479 (1997).
12. C. B. Field, J. T. Randerson, C. M. Malmström, *Remote Sens. Environ.* **51**, 74 (1995).
13. J. L. Monteith, *J. Appl. Ecol.* **9**, 747 (1972).
14. A. Morel, *Prog. Oceanogr.* **26**, 263 (1991).
15. P. J. Sellers, *Remote Sens. Environ.* **21**, 143 (1987).
16. M. J. Behrenfeld and P. G. Falkowski, *Limnol. Oceanogr.* **42**, 1 (1997).
17. W. M. Balch and C. F. Byrne, *J. Geophys. Res.* **99**, 7555 (1994).
18. J.-F. Berthon and A. Morel, *Limnol. Oceanogr.* **37**, 781 (1992).
19. G. Russell, P. G. Jarvis, J. L. Monteith, in *Plant Canopies: Their Growth, Form and Function*, G. Russell, B. Marshall, P. G. Jarvis, Eds. (Cambridge Univ. Press, Cambridge, 1989), pp. 21–39.
20. A. Ruimy, G. Dedieu, B. Saugier, *J. Geophys. Res.* **99**, 5263 (1994).
21. D. Antoine, J. M. Andre, A. Morel, *Global Biogeochem. Cycles* **10**, 57 (1996).
22. W. Balch *et al.*, *J. Geophys. Res.* **97**, 2279 (1992).
23. R. R. Bidigare, B. B. Prezelin, R. C. Smith, in *Primary Productivity and Biogeochemical Cycles in the Sea*, P. G. Falkowski, Ed. (Plenum, New York, 1992), pp. 175–212.
24. G. Joel, J. A. Gamon, C. B. Field, *Remote Sens. Environ.* **62**, 176 (1997).
25. J. Runyon, R. H. Waring, S. N. Goward, J. M. Welles, *Ecol. Appl.* **4**, 226 (1994).
26. C. S. Potter *et al.*, *Global Biogeochem. Cycles* **7**, 811 (1993).
27. Confidence in NPP estimates from these and similar models can be derived from several sources, including ability to reproduce small-scale NPP measurements, model intercomparisons (*11*), fidelity in tracking interannual variations in agricultural NPP over large regions [C. M. Malmström *et al.*, *Global Biogeochem. Cycles* **11**, 367 (1997)], and ability to reproduce the annual cycle of atmospheric CO_2 [W. Knorr and M. Heimann, *Tellus Ser. B* **47**, 471 (1995; J. T. Randerson, M. V. Thompson, I. Y. Fung, T. Conway, C. B. Field, *Global Biogeochem. Cycles* **11**, 535 (1997)], when coupled with appropriate atmospheric and heterotrophic models. Even with these approaches, the actual values still include uncertainties related to both the data and the structure of the models.
28. G. Feldman *et al.*, *Eos* **70**, 634 (1989).
29. J. D. Tarpley, S. R. Schneider, R. L. Money, *J. Clim. Appl. Meteorol.* **23**, 491 (1984).
30. The processed NDVI data set used for this report is from S. O. Los [thesis, Vrije University, Amsterdam (1998)].
31. Until the launch of SeaWiFS in September 1997, there was no single instrument appropriate for estimating APAR in the oceans and on land at the global scale. For the oceans, there has been no color sensor at all since the end of the CZCS mission in 1986. For land, the AVHRR instruments aboard the NOAA satellites have been invaluable, even though their design was not optimized for vegetation monitoring.
32. J. K. B. Bishop and W. B. Rossow, *J. Geophys. Res.* **96**, 16839 (1991).
33. Sea-surface temperatures are climatological averages from the U.S. Navy Marine Climatic Atlas (CD-ROM) (Naval Command Oceanographic Detachment Center, Asheville, NC, 1995), with processing described in (*16*).
34. Terrestrial temperatures were calculated for 1982 to 1990 from long-term averages (*54*) plus anomalies from the updated data set of J. Hansen and S. Lebedeff [*J. Geophys. Res.* **92**, 13345 (1987)]. These temperatures were then averaged by month, for the 9-year period.
35. Terrestrial precipitation was calculated for 1982 to 1990 from long-term averages (*54*) plus anomalies from C. B. Baker, J. K. Eischeid, T. R. Karl, and H. F. Diaz (paper presented at Ninth Conference on Applied Climatology, American Meteorological Society, Dallas, TX, 1995). These values were then averaged by month, over the 9-year period.
36. L. Zobler, A world soil map for global climate modeling (*NASA Technical Memorandum 87802*, NASA, New York, 1986).
37. R. S. DeFries and J. R. G. Townshend, *Int. J. Remote Sens.* **15**, 3567 (1994).
38. This estimate includes a 1 Pg of C contribution from macroalgae [S. V. Smith, *Science* **211**, 838 (1981)]. Differences in ocean NPP estimates in (*16*) and those in Fig. 1 and Table 1 result from (i) addition of Arctic and Antarctic monthly ice masks, (ii) correction of a rounding error in previous calculations of pixel area, and (iii) changes in the designation of the seasons to correspond with (*3*).
39. O. J. Koblentz-Mishke, V. V. Volkovinsky, J. G. Kabanova, in *Scientific Exploration of the South Pacific*, W. S. Wooster, Ed. (National Academy of Science, Washington, DC, 1970), pp. 183–193.
40. G. M. Woodwell *et al.*, *Science* **199**, 141 (1978).
41. This value corresponds to an integrated phytoplankton from the surface to Z_{eu} of about 15 mg m^{-2}.
42. M. V. Thompson and J. T. Randerson, *Global Change Biol.*, in press.
43. G. L. Pickard and W. J. Emery, *Descriptive Physical Oceanography: An Introduction* (Pergamon, Oxford, UK, 1982).
44. Seasonal maps of global NPP are available at www.sciencemag.org/feature/data/982246.shl
45. J. H. Martin, S. E. Fitzwater, R. M. Gordon, *Global Biogeochem. Cycles* **4**, 5 (1990).
46. J. H. Martin, R. M. Gordon, S. E. Fitzwater, *Limnol. Oceanogr.* **36**, 1793 (1991).
47. Over millennial time scales, water and temperature are the dominant controlling factors for terrestrial NPP, with effects of nutrient availability assuming a major role on interannual to decadal time scales (*51*) [D. S. Schimel *et al.*, *Global Biogeochem. Cycles* **10**, 677 (1996)].
48. P. M. Vitousek, H. A. Mooney, J. Lubchenco, J. M. Melillo, *Science* **277**, 494 (1997).
49. On land, but not in the oceans, elevated atmospheric CO_2 could facilitate increased carbon storage per unit of stored nutrients, through increased allocation to recalcitrant tissues with high ratios of carbon to nutrients [G. R. Shaver *et al.*, *Bioscience* **42**, 433 (1992)].
50. D. S. Schimel *et al.*, *Global Biogeochem. Cycles* **8**, 279 (1994).
51. R. H. Braswell, D. S. Schimel, E. Liner, B. Moore III, *Science* **278**, 870 (1997).
52. R. B. Myneni, C. D. Keeling, C. J. Tucker, G. Asrar, R. R. Nemani, *Nature* **386**, 698 (1997).
53. P. Ciais, P. Tans, M. Trolier, J. W. C. White, R. J. Francey, *Science* **269**, 1098 (1995).
54. D. J. Shea, *Climatological Atlas: 1950–1979* (TN-269, National Center for Atmospheric Research, Boulder, CO, 1986).

55. The CASA modeling activity has been supported through NASA's Earth Observing System program as part of an Interdisciplinary Science grant to P. J. Sellers and H. A. Mooney and a grant from the Western Regional Center of the Department of Energy National Institute for Global Environmental Change to C.B.F. The VGPM activity has been supported through NASA grants to P.F. and M.J.B. J.T.R. was supported by a NASA Earth System Science Graduate Student Fellowship. Thanks to A. Lowry, D. Kolber, Z. Kolber, M. Thompson, and C. Malmström for assistance in developing and exercising the models. This is Carnegie Institution of Washington Department of Plant Biology publication 1279.

28 March 1998; accepted 8 June 1998

Abrupt Shift in Subsurface Temperatures in the Tropical Pacific Associated with Changes in El Niño

Thomas P. Guilderson and Daniel P. Schrag

Radiocarbon (^{14}C) content of surface waters inferred from a coral record from the Galápagos Islands increased abruptly during the upwelling season (July through September) after the El Niño event of 1976. Sea-surface temperatures (SSTs) associated with the upwelling season also shifted after 1976. The synchroneity of the shift in both ^{14}C and SST implies that the vertical thermal structure of the eastern tropical Pacific changed in 1976. This change may be responsible for the increase in frequency and intensity of El Niño events since 1976.

Several studies have noted that the pattern of El Niño–Southern Oscillation (ENSO) variability changed in 1976, with warm (El Niño) events becoming more frequent and more intense (*1*). This "1976 Pacific climate shift" has been characterized as a warming in SSTs through much of the eastern tropical Pacific. A recent study (*2*) proposed that this shift originated when a subsurface warm water anomaly in the North Pacific penetrated through the subtropics and into the tropics. This model is consistent with an association of the shift in tropical temperatures with changes in North Pacific sea-level pressures (*3*). However, this interpretation is controversial, and other mechanisms might be responsible. Unfortunately, hydrographic observations have spatial and temporal biases that do not allow for a definitive solution.

To examine changes in the origin of water upwelling in the eastern Pacific during the

T. P. Guilderson, Department of Earth and Planetary Sciences, Harvard University, Cambridge, MA 02138, USA, and Center for Accelerator Mass Spectrometry, Lawrence Livermore National Laboratory, Livermore, CA 94550, USA. D. P. Schrag, Department of Earth and Planetary Sciences, Harvard University, Cambridge, MA 02138, USA.

1970s, we obtained a record of radiocarbon variability ($\Delta^{14}C$) from a coral from the Galápagos Islands (*4*). Skeletal carbonate from coral colonies records the $\Delta^{14}C$ of the dissolved inorganic carbon in the surrounding water and can be used as a tracer of ocean circulation (*5, 6*). Surface waters are enriched in ^{14}C relative to deeper water because of the air-sea exchange with ^{14}C that was produced by the atmospheric testing of nuclear weapons in the 1950s and 1960s. This enrichment difference makes the distribution of ^{14}C very sensitive to vertical mixing. In the Galápagos Islands, $\Delta^{14}C$ values at the surface are affected by the vigor of upwelling and by the origin of upwelling water. Our new $\Delta^{14}C$ time series extends from 1957 through 1982 (ending when the colony died during the 1982–83 El Niño) and has an average resolution of eight samples per year (Fig. 1).

The $\Delta^{14}C$ values increase about linearly from pre-1960 values of −70 to −90 per mil, which is consistent with previous measurements of Galápagos corals (*5, 7*), through maximum values of 60 per mil in 1982. Water samples from nearby locations collected as part of the World Ocean Circulation Experiment (WOCE) program in late March and early April of 1993 give values of ~70 per mil (*8*), implying that surface $\Delta^{14}C$ values have stabilized and may have peaked in this region since 1983. In addition to the long-term trend, the coral record shows large seasonal and interannual variability; low $\Delta^{14}C$ values are measured during July through September, and higher values are measured during January through March. The amplitude of the seasonal cycle increased from 20 to 30 per mil in the early 1960s to 50 to 100 per mil in the mid-1970s. After 1976, the seasonal variability decreased to 40 per mil because the minimum values increased abruptly by ~60 per mil. The rate of increase of $\Delta^{14}C$ during the upwelling season was 4.4 per mil year^{-1} between 1960 and 1976, and the rate decreased to 3.0 per mil year^{-1} thereafter. During the nonupwelling season, these rates were 7.0 per mil year^{-1}, decreasing to 2.2 per mil year^{-1} after 1976.

The patterns of radiocarbon variations in the time series can be explained in terms of variability in the intensity of upwelling and changes in the source water that feeds the upwelling. The upwelling in the eastern tropical Pacific exposes water from the Equatorial Undercurrent, a subsurface water mass that flows from west to east, approximately bounded by potential density surfaces (isopycnals) of 24 and 26 kg m^{-3} (*9*). This water is derived from subduction of surface water in the subtropics and water entrained from greater depths in the tropical thermocline. The subtropical water brings higher bomb-produced ^{14}C levels from the sea surface down into the undercurrent. The entrained component mixes colder, low ^{14}C water into the undercurrent and augments the $\Delta^{14}C$ contrast between the undercurrent and the sea surface (*6, 10*). The deeper component with less bomb-produced ^{14}C is at least as deep as the isopycnal of 26.5 kg m^{-3} (*6, 9*). The time for transport from the subtropics to the tropics is long enough (10 to 20 years) (*11*) that, when coupled with lower gas exchange in the tropics because of lower wind velocities, the peak of bomb-produced radiocarbon in the tropics is delayed relative to the peak in the subtropics (*5, 6*). The maximum $\Delta^{14}C$ values that are reached in the eastern tropical Pacific are lower than those in the subtropical regions because of dilution by the entrained component. Upwelling in July through September, when the thermocline is shallow, brings water from the undercurrent to the surface, lowering $\Delta^{14}C$ values. In January through March, when the thermocline is deeper, surface $\Delta^{14}C$ values increase slightly because of air-sea exchange and lateral advection of off-equatorial high $\Delta^{14}C$ water. The amplitude of the seasonal cycle around the Galápagos Islands increased from 1960 through 1976 because the surface water surrounding the upwelling region responded more quickly to the invasion of bomb-produced ^{14}C than did water in the undercurrent.

Interannual variability in the coral record is dominated by ENSO. During warm events, the depth of the thermocline increases in the east, so that Ekman pumping no longer brings water from the undercurrent to the surface. This creates high $\Delta^{14}C$ anomalies in the coral time series (1965–1966, 1969–1970, and 1972–1973), which are most pronounced from July through September. The increase of over 100 per mil within a few months in 1976 is unusually large in relation to the magnitude of the warm event. The $\Delta^{14}C$ values during upwelling seasons remained anomalously high after this rapid rise. A linear trend through the minimum seasonal $\Delta^{14}C$ values showed a 20 per mil offset in 1976, with no equivalent offset in maximum values (Fig. 1). There was no abrupt change in wind velocities in 1976 that could cause a sudden reduction in upwelling intensity, although it is difficult to interpret wind data because the observed and reconstructed wind fields show differing trends since 1960 (*12*).

The abrupt increase in minimum $\Delta^{14}C$ values occurred when SSTs shifted in the eastern tropical Pacific and the frequency and intensity of ENSO warm phases increased. The shift in average temperature (Fig. 2) has a strong seasonal bias and is similar to the bias shown by the radiocarbon data. For the upwelling season, minimum SSTs were relatively stable and low from 1945 to 1955, and in 7 of 11 years, temperatures were lower than 22.5°C. The highest minimum SSTs were measured during the 1951 and 1953 El Niño events. A break occurred in 1955–1956, and through 1975, minimum temperatures were close to 23.5°C and were never as low as 22.5°C, although this break may be an instrumental artifact (*13*). Minimum SSTs shifted again in 1976 to a minimum value of 24.5°C (ENSO warm events excluded); only 1989 had temperatures that were lower than 23.5°C (*14*). Maximum temperatures (January to March) increased slightly

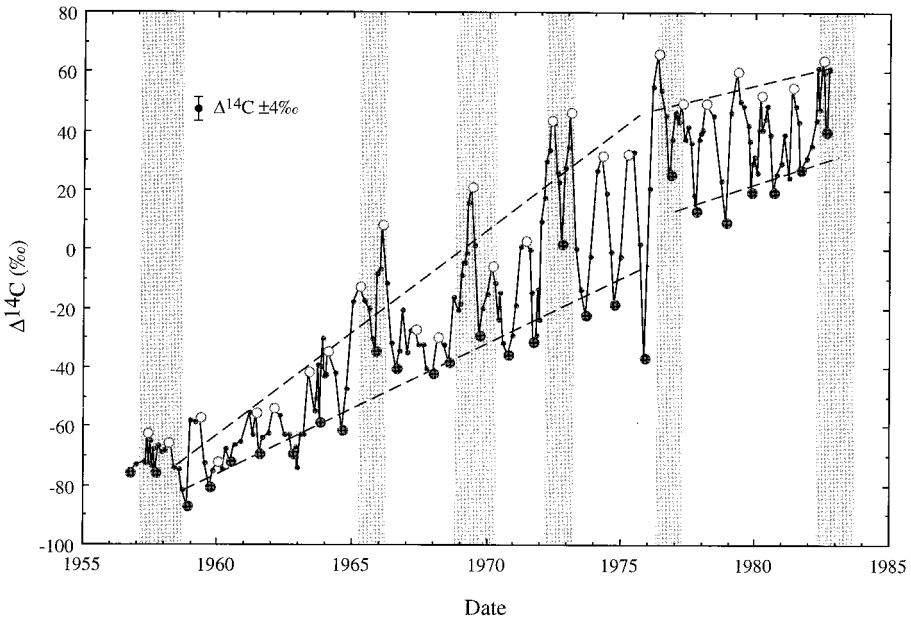

Fig. 1. Galápagos coral $\Delta^{14}C$ [in per mil (‰)] record from 1957 to 1983 (1σ error bars). For reference, WOCE P19 surface measurements for stations near the Galápagos taken from 29 March to 1 April 1993 average 70 per mil (*8*). Upwelling season maxima are indicated by solid circles; nonupwelling season maxima are indicated by open circles. Linear trends of the upwelling and nonupwelling season extremes are shown (dashed lines) (*4*) and are as described in the text. Shaded areas highlight El Niño years when the Niño-3 SST anomaly was ≥1°C.

after 1976 as a result of more frequent ENSO warm phases, with no change occurring in non–El Niño years (*14*).

The restriction of the shift in $\Delta^{14}C$ values and SSTs to the season of the most intense upwelling implies that a persistent shift in temperature and $\Delta^{14}C$ of the subsurface waters in the eastern tropical Pacific occurred in 1976. The $\Delta^{14}C$ data require that the source of the upwelling contained a greater proportion of water with bomb-produced radiocarbon after 1976, presumably from subduction in the subtropics. The simplest way to satisfy the SST and $\Delta^{14}C$ constraints is to alter the vertical density structure along the equator so that the contribution of deeper, colder, lower $\Delta^{14}C$ water to the upwelling region is reduced. A deepened thermocline in the eastern tropics after 1976, superimposed on variations in thermocline depth over seasonal and interannual time scales, is supported by subsurface temperature data (*2*), although the availability of such data before 1976, particularly data from the Southern Hemisphere, is not sufficient to identify more detailed patterns. A deepened thermocline is consistent with overall weaker zonal winds, although the reliability of the wind data, particularly for any long-term trends, is controversial (*12*).

A fundamental question is whether the change in the thermocline depth in 1976 is a contributing cause to the change in the frequency and intensity of El Niño or is merely an effect of the stronger warm events and reduced trade winds. A related question is whether the change predominantly represents a shift in winds affecting the tilt of the thermocline along the equator or a shift in ocean circulation affecting thermocline depth in the east without compensation in the west. Although numerous modeling studies have described the coupling of thermocline depth, wind stress, and El Niño dynamics (*15*), the persistence of warmer SSTs during upwelling seasons since 1976, even during cold phase (La Niña) conditions, suggests that a change in the ocean, independent from wind forcing, might be involved. One such change, suggested by Zhang *et al*. (*2*), involves subduction in the North Pacific of a warm temperature anomaly from the late 1960s and early 1970s. However, Zhang *et al*. note that a cold anomaly in the North Pacific after 1980 should have restored cooler conditions to the eastern tropics, rather than sustaining the warm conditions that have persisted. Furthermore, temperature and salinity data suggest that the South Pacific is the dominant source of water in the undercurrent (*9*) and therefore that the impact of an anomaly in the North Pacific should be minor. The shift at the equator occurred only 8 years after the maximum warm anomaly in the North Pacific, which is a shorter time period than most estimates for the transport time of water between the subtropics and the equator (*11*). A warm anomaly in the North Pacific cannot explain the $\Delta^{14}C$ shift, for the reason that advection of a warm anomaly along isopycnal surfaces would not affect $\Delta^{14}C$ values because $\Delta^{14}C$ is a water mass tracer unaffected by temperature. Thus, our data do not support the Zhang *et al*. hypothesis.

An alternative hypothesis is that the source of the equatorial undercurrent changed and southern water became even more dominant after 1976. This would be expressed as a shift in both temperature and salinity, because South Pacific water from the thermocline is warmer and saltier than North Pacific water along a given isopycnal surface (*9*). Partial support for this hypothesis is given by limited hydrographic data (*16*) showing that the temperature shift in the eastern equatorial Pacific was accompanied by a slight increase in salinity. However, a shift in sources of the undercurrent cannot explain the rise in $\Delta^{14}C$ values, because Southern Hemisphere water, in general, has lower $\Delta^{14}C$ on a given isopycnal surface relative to Northern Hemisphere water (*6, 10*).

Future research should explain why the shifts in temperature and $\Delta^{14}C$ appear as step functions rather than as gradual changes. Earlier step-like transitions are also seen in the SST record (for example, in 1955–1956), but it is not clear if these values are authentic or are an artifact of changes in measurement technique or of scarcity of observations (*13*). Although nonlinear systems exhibit such behavior, there is no existing theory that explains why the processes affecting the vertical structure of the tropical pycnocline should respond in a step-like fashion. Before continuous subsurface monitoring of temperature and salinity in the 1980s, hydrographic data were too sparse to explore this question in detail. It may be possible to obtain data from carbonate-secreting organisms that grow at thermocline depths (for example, sclerosponges and ahermatypic corals) to provide additional constraints on what happened in the ocean in 1976. Additional radiocarbon data on Galápagos corals from times in the past 100 years when the frequency of El Niño is known to have waxed and waned could be used to determine whether similar shifts in thermocline structure occurred at these intervals and whether the "1976 climate shift" was truly unusual.

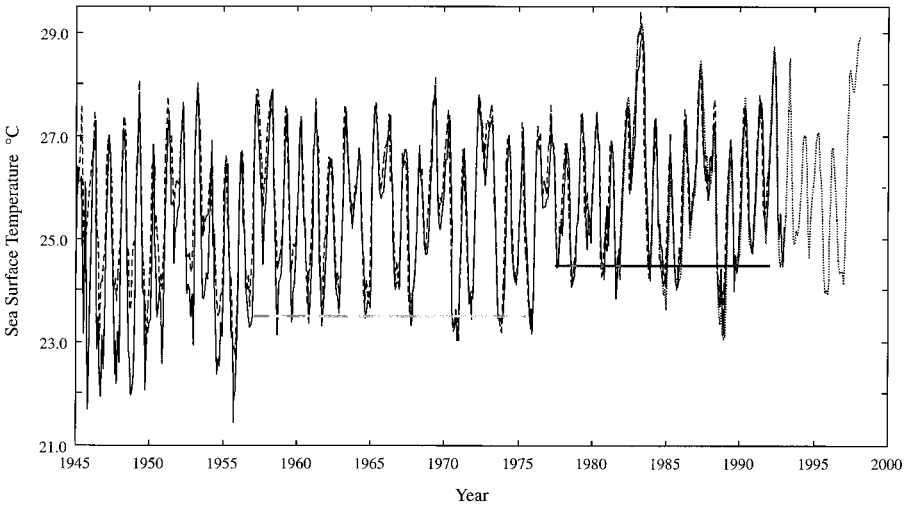

Fig. 2. SSTs in the Niño-3 region (90° to 150°W, ±5°) as observed in COADS (solid line), GOSTA (dashed line), and NMC/IGOSS (dotted line) databases (*20*). Warm season SSTs have remained relatively invariant, whereas upwelling season SSTs underwent a step-like warming in 1976. The horizontal lines indicate average minimum temperatures excluding strong El Niño years (Niño-3 SST anomaly ≥ 1.25°C) for the periods 1955–1975 and 1976–1992.

References and Notes

1. K. Y. Trenberth and T. J. Hoar, *Geophys. Res. Lett.* **23**, 57 (1996); B. Rajagopalan, U. Lall, M. Cane, *J. Clim.* **10**, 2351 (1997).
2. R.-H. Zhang, L. M. Rothstein, A. J. Busalacchi, *Nature* **391**, 879 (1998); see also C. Deser, M. A. Alexander, M. S. Timlin, *J. Clim.* **9**, 1840 (1996); D. Gu and S. G. H. Philander, *Science* **275**, 805 (1997).
3. A. Kumar, A. Leetmaa, M. Ji, *Science* **266**, 632 (1994); K. Y. Trenberth and J. W. Hurrell, *Clim. Dyn.* **9**, 303 (1994); J. M. Wallace, Y. Zhang, L. Bajuk, *J. Clim.* **9**, 249 (1996); Y. Zhang, J. M. Wallace, D. S. Battisti, *ibid.* **10**, 1004 (1997).
4. Cores of a *Porites* colony from Urvina Bay, Isabella Island, Galápagos Archipelago, were collected by J. Wellington and supplied to us by R. Dunbar. The westward side of Urvina Bay faces the open ocean and is therefore a representative location for documenting the regional upwelling signal. The coral was sampled along the major growth axis at 2-mm increments with a low-speed drill. Splits (~1 mg) were reacted in vacuum in a modified autocarbonate device at 90°C, and the purified CO_2 was analyzed on a gas-source stable isotope ratio mass spectrometer to obtain oxygen and carbon isotopic data. The remaining sample splits (7 mg) were placed in individual reaction chambers, evacuated, heated, and acidified with orthophosphoric acid. The evolved CO_2 was purified, trapped, and converted to graphite in the presence of a cobalt catalyst in individual reactors (*17*). Graphite targets were measured at the Center for Accelerator Mass Spectrometry, Lawrence Livermore National Laboratory (*18*). Radiocarbon results are reported as $\Delta^{14}C$ (units are per mil) as defined by Stuiver and Polach (*19*) and include the $\delta^{13}C$ correction using the stable isotope results. The external

precision of the radiocarbon measurements is ±4 per mil (1σ). The age model is derived from a linear interpolation procedure between the oxygen isotope results and the instrumental SST record in the Galápagos Islands by matching peaks and troughs, with an estimated error of less than 3 months. Linear trends of upwelling and nonupwelling season extremes were determined for the 1960–1975 and 1976–1983 periods and were offset by 20 per mil for the upwelling season. We did not include the 1975 upwelling nor the 1976 warm season extremes, in order to unbias the trends.
5. E. M. Druffel, *Geophys. Res. Lett.* **8**, 59 (1981).
6. J. R. Toggweiler, K. Dixon, W. S. Broecker, *J. Geophys. Res.* **96**, 50 (1991).
7. E. M. Druffel, *J. Mar. Res.* **45**, 667 (1987).
8. National Ocean Sciences Accelerator Mass Spectrometry Facility, *NOSAMS Report 94-109, WOCE AMS ^{14}C Data Report 4* (Woods Hole, MA, 1994) (courtesy of R. Key).
9. K. Wyrtki and B. Kilonsky, *J. Phys. Oceanogr.* **14**, 242 (1984); M. Tsuchiya, R. Lukas, R. A. Fine, E. Firing, E. Lindstrom, *Prog. Oceanogr.* **23**, 101 (1989); Y. Gouriou and J. Toole, *J. Geophys. Res.* **98**, 22495 (1993).
10. P. D. Quay, M. Stuiver, W. S. Broecker, *J. Mar. Res.* **41**, 769 (1983); R. M. Key *et al.*, *Radiocarbon* **38**, 425 (1996).
11. R. A. Fine, J. L. Reid, H. G. Ostlund, *J. Phys. Oceanogr.* **11**, 3 (1981); M. J. McPhaden and R. A. Fine, *ibid.* **18**, 1454 (1988); R. A. Fine, R. Lukas, F. M. Bingham, M. J. Warner, R. H. Gammon, *J. Geophys. Res.* **99**, 25063 (1994); Y. W. Watanabe, K. Harada, K. Ishikawa, *ibid.* p. 25195; M. J. Warner, J. L. Bullister, D. P. Wisegarver, R. H. Gammon, R. F. Weiss, *ibid.* **101**, 20525 (1996).
12. D. S. Luther and D. E. Harrison, *Mon. Weather Rev.* **112**, 285 (1984); A. J. Clarke and A. Lebedev, *J. Clim.* **9**, 1020 (1996); *ibid.* **10**, 1722 (1997).
13. The early shift in 1955–1956 could be the result of poor spatial coverage and instrumental bias while SST measurement techniques migrated from bucket measurements to engine intake measurements [T. P. Barnett, *Mon. Weather Rev.* **112**, 303 (1984)]. The Comprehensive Ocean-Atmosphere Data Set (COADS) database does not attempt to correct for potential instrumental biases, whereas the Global Ocean Surface Temperature Atlas (GOSTA) database does.
14. We performed a pooled *t* test of the means of the warm and upwelling seasons for the Niño-3 region using both the COADS and GOSTA databases for the periods 1956–1975 and 1976–1992. Mean upwelling SSTs are significantly different ($P < 0.01$) for both data sets. Warm season SSTs are nearly identical in the two time periods. Slight differences between data sets exist in terms of absolute SST and magnitude of change relative to the shift in 1976. However, in both data sets, mean coldest month SSTs shift 0.6° (GOSTA) to 1.0° (COADS) in relation to their post-1955 intervals.
15. S. E. Zebiak and M. A. Cane, *Mon. Weather Rev.* **115**, 2262 (1987); N. E. Graham and W. B. White, *Science* 240, 1293 (1988) and references therein.
16. We examined hydrographic profiles (2°N to 2°S, 85° to 110°W) that are archived in the Scripps Institute of Oceanography, National Oceanographic Data Center (NODC) SD2 database. Although there are not enough profiles to create seasonally resolved composite profiles, there is a consistent increase in subsurface salinity and potential temperature after 1976. The salinity increase is not enough to offset the impact of high temperatures on subsurface density. In the conductivity-temperature-depth database, the subsurface warming maxima (1.2°C) is between 40 and 80 dbar and extends to depths >300 dbar. Analysis of all available temperature data [expendable bathythermograph, mechanical bathythermograph, Integrated Global Ocean Station System (IGOSS) radio message bathythermograph, and Nansen casts archived at NODC] shows a similar profile with the subsurface temperature maximum difference of 1.6°C. The warming is persistent irrespective of the inclusion of years with strong El Niño events.
17. J. S. Vogel, J. R. Southon, D. E. Nelson, *Nucl. Instrum. Methods Phys. Res. Sect. B* **29**, 50 (1987).
18. J. C. Davis *et al.*, *ibid.* **52**, 269 (1990).
19. M. Stuiver and H. A. Polach, *Radiocarbon* **19**, 355 (1977).
20. COADS database: S. D. Woodruff, R. J. Slutz, R. L. Jenue, P. N. Steurer, *Bull. Am. Meteorol. Soc.* **68**, 521 (1987); GOSTA database: M. Bottomley, C. K. Folland, J. Hsiung, R. E. Newell, D. E. Parker, *Global Ocean Surface Temperature Atlas (GOSTA)* (U.K. Meteorological Office, Bracknell, United Kingdom, 1990); U.S. National Meteorological Center (NMC)/IGOSS database: R. W. Reynolds and T. M. Smith, *J. Clim.* **7**, 929 (1994).
21. This manuscript benefited greatly from discussions with M. Cane, G. Philander, K. Rodgers, and S. Trumbore. The authors thank M. Kashgarian, J. Southon, and E. Goddard for assistance. Critical comments and reviews were provided by E. Druffel, W. Jenkins, and two anonymous reviewers. This work was supported by a grant from NSF's program in Physical Oceanography (OCE-9796253) and by grants from the Lawrence Livermore National Laboratory (98-ERI-002 and a Center for Accelerator Mass Spectrometry minigrant). Radiocarbon analyses were performed under the auspices of the U.S. Department of Energy by the Lawrence Livermore National Laboratory (contract W-7405-Eng-48). Data will be digitally archived at the Carbon Dioxide Information Analysis Center (Oak Ridge, TN) and the World Data Center A (Boulder, CO).

30 March 1998; accepted 8 June 1998

Solidus of Earth's Deep Mantle

A. Zerr, A. Diegeler, R. Boehler

The solidus of a pyrolite-like composition, approximating that of the lower mantle, was measured up to 59 gigapascals by using CO_2 laser heating in a diamond anvil cell. The solidus temperatures are at least 700 kelvin below the melting temperatures of magnesiowüstite, which in the deep mantle has the lowest melting temperatures of the three major components—magnesiowüstite, Mg-Si-perovskite, and Ca-Si-perovskite. The solidus in the deep mantle is more than 1500 kelvin above the average present-day geotherm, but at the core-mantle boundary it is near the core temperature. Thus, partial melting of the mantle is possible at the core-mantle boundary.

The solidus of a multicomponent system relevant to that of the lower mantle plays a fundamental role for modeling the early evolution of the Earth and for understanding seismic anomalies in the D″-layer at the core-mantle boundary (CMB). Both temperature and composition of a partial melt at the solidus cannot be accurately predicted even if the melting temperatures of the end members are known. For example, it is difficult to reconcile recent findings from seismic data which suggest partial melting in the lowermost part of the mantle (*1*), with measurements in laser-heated diamond cells which have shown that the melting temperature of $(Mg,Fe)SiO_3$-perovskite, previously thought to be near the eutectic (*2*), increases rapidly with pressure (*3, 4*). The melting curve of magnesiowüstite, (Mg,Fe)O, the second most abundant lower mantle mineral, however, has a much smaller slope (*5*), and this difference in the melting behavior of the end-member components complicates the predictions of the eutectic temperature and eutectic composition in the lower mantle.

Only a few melting experiments have been done on compositions that may approximate those of the lower mantle, and these were not conducted at pressures above 25 GPa (*6, 7*). The melting temperature of olivine has been estimated at 4300 ± 270 K at about 130 GPa from a shock-wave experiment (*8*). This result provides a constraint on the binary eutectic temperature between magnesiowüstite and $(Mg,Fe)SiO_3$-perovskite. Here we describe results from measurements of the solidus temperature for a multiphase mantle-like composition over a pressure range equivalent to depths of 600 to 1500 km in the Earth (the CMB is at about 3000 km).

We used a glass approximating the composition of pyrolite (*9*) as starting material (*10*). A thin section of this glass sample with typical dimensions of 70 by 70 by <15 μm and a surface roughness of <150 nm was embedded in a diamond cell in argon, which provided inert, thermally insulating, and hydrostatic conditions. We used the CO_2-laser heating technique described elsewhere (*11*). Pressures were measured at room temperature from ruby chips located near the edge of the sample chamber. After heating, the pressure distribution throughout the pressure chamber was nearly uniform (*12*). Because of the small ratio between the volumes of the sample and pressure medium, the thermal pressure was negligible (*11*).

The quenched samples were examined by Raman spectroscopy while still at high pressure to check whether the glass had transformed to a high-pressure phase assemblage. In experiments at pressures less than 22 GPa, the spectra resembled those of β or γ-Mg_2SiO_4 plus Mg-SiO_3-majorite, the major phases of the transition zone. The Raman spectra of these high-pressure phases are unaffected by their Fe or Al contents (*13*). Of the three major lower mantle phases that would be expected to form in our

A. Zerr and R. Boehler, Max-Planck-Institut für Chemie, Postfach 3060, 55020 Mainz, Germany. A. Diegeler, Institut für Mineralogie und Geochemie der Universität zu Köln, 50674 Köln, Germany.